

A Study of Production of Tungsten Copper Alloy by Powder Metallurgy, Applied to Radioactive Shielding of Transport Equipment for Pharmaceutical Products

Francisco Carlos Cione¹, fceoni@usp.br; Armando Cirilo de Souza¹, armandocirilo@yahoo.com;
Frank Ferrer Sene¹, ffsene@hotmail.com; Márcia de Almeida Rizzutto², marizzutto@if.usp.br;
Jesualdo Luiz Rossi¹, (jelrossi@ipen.br)

¹IPEN - Instituto de Pesquisas Energéticas e Nucleares, IPEN-CNEN/SP - Av. Lineu Prestes, 2242, São Paulo, 05508-000 Brazil

²IFUSP - Instituto de Física da Universidade de São Paulo, Rua do Matão, s/n, São Paulo, Brazil

Abstract

Safety is of paramount importance for the storage and transportation of radiopharmaceutical products, being directly dependent on the radiation shielding material used in specific devices. The focus of present work, part of a larger project, is to minimize the use of harmful materials, as lead and depleted uranium, in such devices construction. The radioactive energy reduction varies according to density of material used as shielding. Because Tungsten has a high density and, implicitly, good shielding properties without to be harmful, but has poor workability, researches were focused on Tungsten - copper heavy alloys. The objective of the performed research was the optimization of alloy composition in order to achieve the best linear absorption coefficient. The studied compositions were 15, 20 and 25 wt.% copper. The linear absorption coefficient was similar either for the green and sintered compacts, thus the porosity level did not have measurable effect on the radiation attenuation.

1. Introduction

Radiation is a serious concern in nuclear power facilities, industrial or medical x-ray systems. Preserving both human safety and structural material that may be compromised from radiation exposure are vital. This is realized by radiation shielding, based on the principle of attenuation - ability to reduce a wave's or ray's effect by blocking or bouncing particles through a barrier material [1]. Appropriate equipment, provided with liners or walls from efficient shielding materials [2], e.g. hermetic closed boxes, sharp containers, vials, mobile radiation shields etc. (Fig. 1) is used for this purpose. Selection of shielding material must take into consideration the attenuation effectiveness – depending on the type of radiation, strength, resistance to damage, thermal properties and cost efficiency [2]. Charged particles may be attenuated by losing energy to reactions with electrons in the barrier, while x-ray and gamma radiation are attenuated through photoemission, scattering, or pair production [2],[4].

The most used in radiopharmaceutical products are sources of gamma-ray radiation [5]. The gamma-ray attenuation by the shielding (absorber) material follows an exponential law. So, when a gamma radiation of intensity I_0 is incident on an absorber of thickness L , the intensity (I) transmitted through the absorber is given by the exponential relation:

$$I(L) = I_{(0)} \cdot e^{(-u_e \cdot L)} \quad (1)$$

where (u_e) is the linear attenuation coefficient (expressed in cm^{-1}) [6]. Its values depend on the absorber material density, i.e., for the same material has different values function of its state (e.g. bulk solid, porous solid, smelted, vapours). Consequently, the attenuation property of a material is more accurately expressed by the mass attenuation coefficient, $u = u_e/\rho$ [cm^2/g]. It quantifies the gamma-ray



Fig. 1. Examples of equipment used in radiation shielding [3].

interaction probability of a given element, irrespective of its state and, consequently, it is usually tabulated [7]. In this case, the above relation becomes:

$$I_{(X)} = I_{(0)} \cdot e^{(-u_e \cdot X)}; \quad I_{(X)} = I_{(0)} \cdot e^{(-u \cdot \rho \cdot L)} \quad (2)$$

where $\rho \cdot L = X$, represents the effective attenuation thickness of the considered material having the physical thickness L [8]. The ratio $I_{(X)}/I_{(0)}$ is called the gamma-ray transmission. However, the direct measurements lead to values of the linear attenuation coefficient, not of the mass one. The reciprocal of the linear attenuation coefficient $1/u_e$ has units of length and is often called the mean free path. The mean free path is the average distance a gamma ray travels in the absorber before interacting. The experiments have shown that the transmission increases with increasing gamma-ray energy and decreases with increasing the effective absorber thickness (X) and also that the linear attenuation coefficient (u_e) depends on the gamma-ray energy, on the atomic number (Z) and on density (ρ [g/cm^3]) of the absorber [4], [6]. That's why as shielding materials are used especially metals of a high density and high atomic number, nowadays the most used being lead ($\rho = 11.35 \text{ g}/\text{cm}^3$ and $Z = 82$, relatively inexpensive and mouldable into many shapes but of less shape stability) [2],[4], [6], [8] and, more recently, depleted uranium ($\rho \approx 19 \text{ g}/\text{cm}^3$, $Z = 92$) [9]. However, both are harmful materials. So, in spite of their shielding efficiency, the limitation of their use, especially of depleted uranium – more dangerous than lead - is an important concern of the health and environment protection [4]. Tungsten, having a significantly higher density than both ($19.35 \text{ g}/\text{cm}^3$) and a quite high atomic number $Z = 74$, seems to be the best alternative to these hazardous materials. Even if it is more expensive, its cost can be compensated, to a certain extent, by the smaller physical layer thickness than of lead for shielding necessary to assure the same attenuation [6]. However, due to the very high melting point ($3422 \text{ }^\circ\text{C}$), its obtaining from ores is more convenient as a powder, while its further processing to bulk metal necessary for shielding possible by Powder Metallurgy (PM) - also difficult and expensive [10]. Therefore, its use for shielding purposes need an adhesion element to make the system properly mouldable, e.g. by inclusion in polymers {e.g. T-Flex® W (88% by mass W)} [4], in so called Lead Free Radiation Shielding [11]}, or in tungsten heavy alloys. Even are more expensive, they are more efficient, usable for more complex/precise equipment, of a much longer lastingness.

There are several classes of heavy alloys, the main, W-Ni-Fe, W-Ni-Co, W-Ni-Cu and W-Cu [12], having, beside shielding, numerous other applications [12],[13]. Their manufacturing is possible only by PM and consists of cold uniaxial / isostatic compaction of powder components mixture to green compacts, sintered in dry hydrogen or inert atmosphere [14]. The commonly used compositions and properties are given e.g. in ref. [12], the most used being W-Ni-Fe. Even if their sintering can be performed in solid state, to obtain the best properties, it must be realized with liquid phase, at $1470 \div 1580 \text{ }^\circ\text{C}$. Beside densification, a continuous network of nearly spherical tungsten particles embedded by diffusion in a Ni-W-Fe matrix, along with precipitates of Fe_3W_2 , Ni_4W or $[\text{Fe,Ni}]_7\text{W}_6$ along the W-matrix boundaries form [12],[15], determining the alloy strengthening but also its embrittlement - decreasing ductility and workability [15]. As the use to radiation shielding devices (see Fig. 1) mostly require sheets or plates, their obtaining by rolling encounters difficulties [12]. So, W-Ni-Cu alloys, also cited in [6], of a Ni-Cu more ductile matrix, are preferred. Instead, even in this case, a liquid phase sintering at over $1350 \div 1400 \text{ }^\circ\text{C}$ is necessary [16], being difficult to avoid compact distortions and Ni-W precipitates formation - with alloy embrittlement [15].

Beside these impediments, in both cases, liquid phase sintering requires high temperature furnaces, implying high costs [12], to which must be added those of subsequent working operations.

For these reasons, W-Cu alloys – the cheapest and of highest workability among tungsten heavy alloys - have been adopted in this first step of investigation. However, since tungsten and copper are insoluble together, they form rather a composite, not a true alloy [12],[16]. Consequently, they are also manufactured through PM, by several possible methods: tungsten skeleton infiltration with molten copper [12], solid state and liquid phase sintering [12]. Beside low productivity, the first allows the obtaining of small relative densities ($30 \div 40 \%$) [12] - not enough for radiation shielding [6]. The simplest and of highest productivity is, certainly, the common PM route – cold compaction of W-Cu powder mixture - solid state sintering [12]. However it also cannot lead to much higher densities, while liquid phase sintering involves inconveniences like the molten Cu leaking from compact or, at least, its distortion [18]. Numerous researches have been performed to avoid them. Among these must be mentioned optimization of W-Cu powder mixture from the particle size and homogeneity points of view [19], of heating mode and of Cu content [20], use of nanocrystalline W-Cu powder – even followed by the compact spark plasma sintering [21], controlled Mechanical Alloying/Milling to increase the powder energetic state of and, implicitly, its sinterability [22],[23]. This last method – the simplest and, certainly, cheapest, has been adopted in the present step of researches. So, they were conducted to produce $X\%W+Y\%Cu$ composites by PM, alternative to presently used lead and depleted uranium as Gamma ray shielding materials and to establish their linear attenuation coefficient variation with composition.

2. Experimental

2.1. W-Cu alloys elaboration

W-Cu compositions considered adequate for radiation shielding but also as having a good behaviour at solid state sintering, i.e. with 15, 20 and 25 wt.% Cu [4],[12],[24] were adopted in this step of researches, realized using commercial W and Cu powders. Because their characteristics were not strictly presented by the producer, particle size distribution were analyzed with a CILAS equipment. The powder mixtures, in sets of the selected compositions, were prepared in agreement to the above-mentioned selected variant. So, after the component preliminary blending in a Turbulla blender for 10 min, to increase their energetic state, each mixture underwent a 30 min Mechanical Milling (MM) in a rotating ball mill, with stainless steel balls of 55 mm diameter, in a powder/ball weight ratio of 1:5 and rotating speed of mill vial of 90 rpm. Because, due to the difference in hardness, the W and Cu particles could suffer different flattening/fracturing degrees, to assure a good mixture homogeneity, after the milling process, the homogenization was continued, again in Turbulla blender, for 90 min. From the as obtained sets of powder mixtures, three green samples for each composition, of the nominal diameter 25.4(+/-0.2) mm and thickness of 9.7(+/- 0.2) mm, were axially pressed with die wall lubrication, on an axial hydraulic press, with 250 MPa and subsequently subjected to isostatic pressing with 250 MPa to increase compact densities. Sintering of all samples has been performed in a continuous, belt furnace, in solid state, at 980 °C – a temperature higher than that commonly used for copper compacts sintering [12] - for 120 min, in a mixture of 90-10 vol. % high purity (class 5.0) hydrogen-nitrogen atmosphere, at a pressure of 1.1 atm, followed by cooling in the water jacked zone of the furnace, with a medium cooling rate of ~15 °C/min. The obtained compacts were characterized in terms of density – necessary in the attenuation coefficient determination - and microstructure.

2.2. Characterization of the obtained alloys concerning properties of radiation shielding

Value of the linear attenuation coefficient can be calculated from relation (1), determining the value of $I_{(L)}$ for a selected value of $I_{(0)}$ and L (thickness of the considered sample). For this purpose, an experimental set up, based on principle from Figure 2, has been realized. It consisted of a radioactive Co^{60} source of a scintigraphy detector and an analogue to digital converter for separation power per channel and counting of photons in each channel (intensity) (Fig. 3).

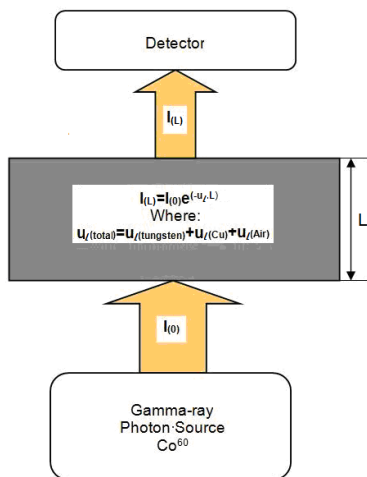


Fig. 2. Principle of the experimental set up for the linear attenuation coefficient measurement.

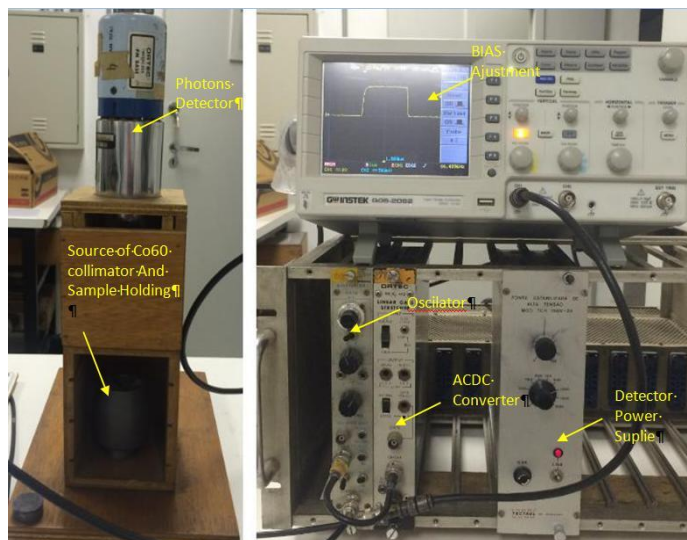


Fig. 3. Experimental set-up realized according to the principle from Fig.4. showing the main used equipments and their connection.

The first step adopted for the experimental assay was to measure the maximum emission value of the radiation source, without absorbing material between the emission source and detector ($I_{(L)}/I_{(0)} = 1$). Subsequently, the obtained set of samples, of selected compositions, were successively mounted in the specially provided fixture of the equipment and measured the transmitted intensities, ($I_{(L)}$).

3. Results and discussion

3.1. Determination of the actual particle size distribution of the used powder

In Figure 4 are presented determined diagrams showing the actual particle size distribution of the used powders, while their medium particle size and purity (given by producer) - in Table 1.

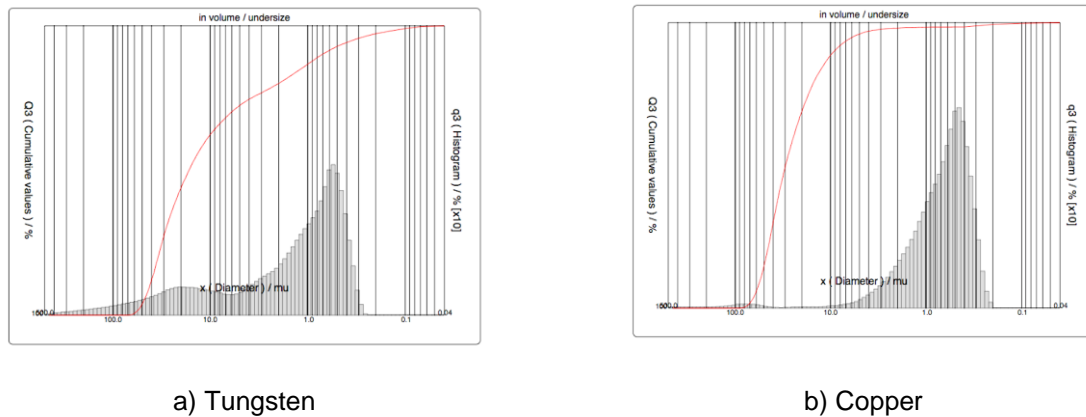


Fig. 4. Experimental diagrams showing particle size distribution of the used powders.

As can be seen, both used powders have a relatively small medium particle size, being fine powders, especially tungsten - which contains a notable proportion of smaller particles than the medium one. Even the medium diameter of particles is bigger at copper powder (Tab. 1), but it is to be

Table1. The main characteristics of the used tungsten and copper powders.

Powder	Medium particle diameter, d_{50} (μm)	Purity (mass %)
W	16.6	98.0
Cu	29.7	99.9

expected that, during the MM process, will suffer a pronounced flattening and cold hardening, followed by a certain fragmentation. Concerning purity, it can be satisfactory for both powders.

3.2. Characterization of the obtained samples

The optical images of typical microstructure of the obtained samples are given in Figure. 5. As can

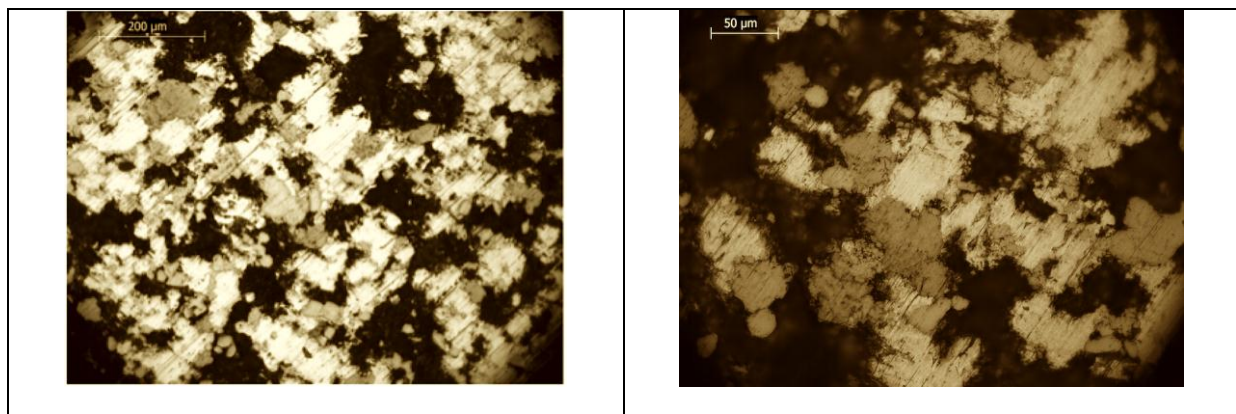


Fig. 5. Optical micrographs of the unetched sample 75W25Cu, of two magnifications.

be seen, they reveal a quite high porosity, with particles that preserved, to a high extent, their initial dimensions and even shapes. This had to be expected taking into consideration that components are totally insoluble and Cu content was too small and its powder particle size too big to allow formation of a continuous matrix, able to encapsulate the W particles. Consequently, the resulted relative densities have quite small values. Because they determine the linear attenuation coefficient of material, have been included in Table 3, beside the determined shielding characteristics.

3.3. Results of the linear attenuation coefficient, (u_e), determination

Determination of the maximum emission value ($I_L/I_{(0)} = 1$) without absorbing material between the emission source and detector (Fig. 6) showed maximum intensity of Co^{60} source in two distinct energy peaks: peak of 957 photons with 1130 keV of energy and 701 photons with 1330 keV of energy. To increase the results accuracy, tests were repeated twice at 5 min interval (see Fig.)

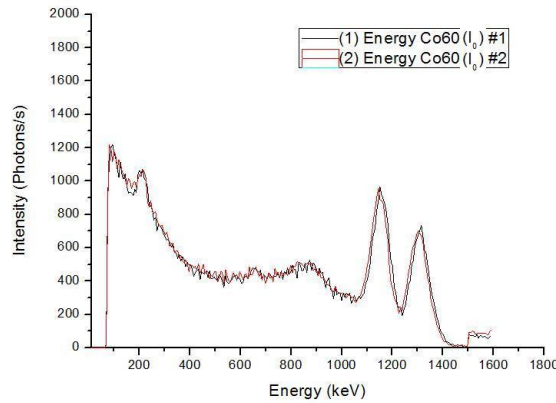


Fig. 6. Free path for Co^{60} radiation emissions in air.

In the graph from Figure 7 one can be visually compared the values of attenuation between the peaks

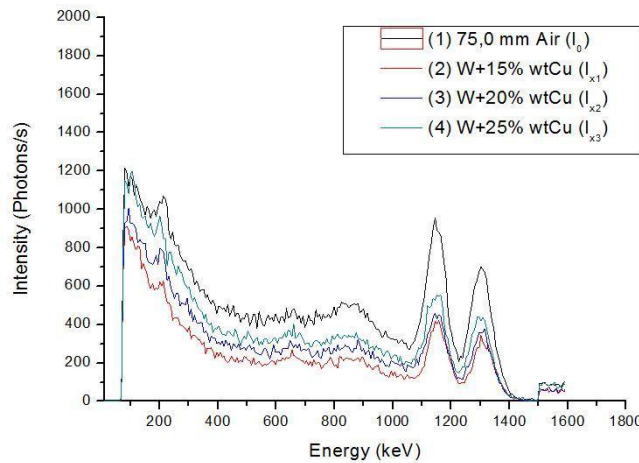


Fig. 7. Radiation Intensity absorption function of its Energy, for the adopted sample compositions..

of each sample containing 15%, 20% and 25% by mass of copper with respect to the peak of maximum intensity ($I_{(0)}$). Table 2 shows the intensity values (I_L) for each peak energy, sample composition and density, along with the calculated values of the linear attenuation coefficients.

Table 2. Determined average linear absorption coefficient function of the tungsten content of samples.

Sample	Density, ρ (g/cm ³)	$I(0)$	$I(L)$	u_e (cm ⁻¹)	Energy (keV)
W+15%Cu	50.3	957	358	9.701	1164
W+20%Cu	53.9	963	438	7.864	1145
W+25%Cu	50.7	948	555	6.341	1138
W+15%Cu	50.3	701	207	4.824	1305
W+20%Cu	53.9	712	324	4.107	1302
W+25%Cu	50.7	709	381	3.780	1319

The attenuation data are conclusive, showing that the sample with the larger tungsten content develops higher attenuation of radiation than the samples with higher content of copper. For the

source of Co^{60} the energy values are close to that which will be imposed against the radiation shield, for the transportation of the pair of radionuclides ^{99}Mo - $^{99\text{m}}\text{Tc}$. Thus one can use these experimental values to obtain more accurately the attenuation coefficient for Mo^{99} .

4. Conclusions

To improve the solid state sinterability of W-Cu heavy alloys, a much finer Cu powder is necessary, along with a coarser W powder. Also, a more efficient process of Mechanical Milling, which has to be performed in Ar atmosphere, using smaller and of different diameter balls, in such a way to get W particles evenly coated by Cu. Powder mixture compaction must be realized with a higher pressure, while sintering at a higher temperature and in an atmosphere with a dew point of minimum $-35\text{ }^{\circ}\text{C}$. Finally, a W-Ni-Cu composition (see, e.g. ref. [6]) would lead to higher densities/shielding properties, but with liquid phase sintering. Finally, longer sintering times can increase determination accuracy.

Acknowledgment: The authors are thankful to Dr. Takiishi H, and Dr. Leal Neto RM for laboratory experiments. The authors are grateful to CAPES (Process 2058/2012) for awarding a scholarship to Cione FC.

References

- [1] * * * Radiation Protection Basics. http://www.epa.gov/radiation/understand/protection_basics.html.
- [2] * * * Materials Used in Radiation Shielding, <http://www.thomasnet.com/articles/custom-manufacturing-fabricating/radiation-shielding-materials>.
- [3] <http://www.biodex.com/nuclear-medicine/products/shielding-storage>.
- [4] D. R. McAlister, Gamma Ray Attenuation Properties of Common Shielding Materials. PG Research Foundation, University Lane Lisle, IL 60532, USA, 2013, <http://www.eichrom.com/PDF/gamma-ray-attenuation-white-paper-by-d.m.-rev-4.pdf>.
- [5] * * * Gamma Radiation, <http://medical-dictionary.thefreedictionary.com/gamma+radiation>.
- [6] G. Nelson, D. Reilly, Gamma-Ray Interactions With The Matter, Los Alamos Laboratories, California - USA, 2010.
- [7] * * * National Institute of Standard and Technology, Physical Measurements Laboratory, XCOM Photon Cross-Sections Database, <http://physics.nist.gov/PhysRefData/Xcom/html/xcom1.html>.
- [8] G. E. Chabot, Shielding of Gamma Radiation. Health Physics Society ed., https://hps.org/documents/shielding_of_gamma_radiation.pdf.
- [9] A. Bleise, P.R. Danesi, W. Burkart, Properties, use and health effects of depleted uranium (DU): a general overview. Journal of Environmental Radioactivity 64 (2003) 93–112.
- [10] * * * Information on tungsten: sources, properties and uses, Internat. Tungsten Industry Assoc., <http://www.itia.info/metal-of-powder-metallurgy.html>.
- [11] * * * <http://www.ecomass.com/radiation-shielding/>.
- [12] S.G. Caldwell, Powder Metallurgy Tungsten Heavy Alloys. In ASM Handbook, vol. 7 - *Powder Metal Technologies and Applications*, ASM International, Ohio, USA, 1998.
- [13] * * * <http://www.wolfmet.com/applications>.
- [14] R.M. German, Liquid Phase Sintering. Springer Science & Business Media, 2013, 244 p.
- [15] B. C. Muddle, Interphase boundary precipitation in liquid phase sintered W-Ni-Fe and W-Ni-Cu alloys. Metallurgical Transactions A Volume 15, Issue 6, 1984, pp 1089-1098.
- [16] Y. Wu, R. M. German, B. Marx, P. Suri, and R. Bollina, Comparison of densification and distortion behaviors of W-Ni-Cu and W-Ni-Fe heavy alloys in liquid-phase sintering," Journal of Materials Science, vol. 38, no. 10, 2003, pp. 2271–2281,
- [17] Upadhyaya, Fabrication of tungsten-copper composites through liquid phase sintering, Transactions of the Indian Institute of Metals, vol. 55, 2002, pp. 51–69,
- [18] S. Eroglu, T. Baykara, Effects of powder mixing technique and tungsten powder size on the properties of tungsten heavy alloys, J. of Mat. Processing Techn. Vol. 103, Iss. 2, 2000, pp.288–292.
- [19] A. Mondal, A. Upadhyaya and D. Agrawal, Effect of Heating Mode and Copper Content on the Densification of W-Cu Alloys, Indian J. of Mat. Science Vol. 2013 (2013),doi.org/10.1155/2013/603791.
- [20] A. Elsayed et al., Experimental investigations on the synthesis of W–Cu nanocomposite through spark plasma sintering, Journal of Alloys and Compounds, (639), 2015, 373–380.
- [21] S.S. Ryu, Y.D. Kim, I.H. Moon, Dilatometric analysis on the sintering behavior of nanocrystalline W–Cu prepared by mechanical alloying, Journal of Alloys and Compounds 335 (2002) 233–240.
- [22] J. S. C. Jang, et al., Study on the solid-phase sintering of the nano-structured heavy tungsten alloy powder, Journal of Alloys and Compounds, 434-435 (2007), 367–370.

Reproduced with permission of the copyright owner. Further reproduction prohibited without permission.